MODE I FRACTURE IN CONCRETE USING CRACK LINE WEDGE LOADED DOUBLE CANTILEVER BEAM

CLWL-DCB試片을 使用한 콘크리트의 開口型 破壞

宋 錠 根*
Song, Jeong Geun

요 약

콘크리트에 線型破壞力學의 適用可能性을 硏究한 많은 論文이 發表되었다. 本 論文에서는 CLWL-DCB 試片을 利用한 콘크리트의 開口型破壞를 硏究하였다.

表面龜裂길이는 리프리카를 使用하여 直接的인 方法으로 測定하였고, 이 結果는 實驗에서 얻은 測定荷重과 龜裂開口變位의 關係曲線을 利用하여 分析하였다. 臨界應力強度係數와 臨界龜裂先端變位는 Two Parameter 모델을 使用하여 有效龜裂先端에서 求하였다.

LEFM 龜裂斷面과 實驗으로 求한 龜裂斷面으로부터 閉鎖壓力을 얻기 爲하여 중첩법을 適用하여 5種의 균열모델을 評價하였다.

ABSTRACT

Many works have been conducted to examine the applicability of linear elastic fracture mechanics to concrete. In this paper, the mode I fracture of concrete is studied using crack line wedge loaded-double cantilever beam(CLWL-DCB) specimen. Surface crack length was directly measured by replica film. The results were analyzed using the measured load versus crack opening displacement response of specimen. Critical stress intensity factor and critical crack tip opening displacement were calculated at the tip of the effective crack using the two parameter model.

The superposition method applied to obtain the closing pressure necessary to match LEFM crack profiles with experimental crack profiles. Five cohesive crack models were evaluated.

Introduction

Although the fundamental concepts of linear elastic fracture mechanics(LEFM) have been successfully applied to a wide range of materials, there is considerable disagreement as to whether these fracture concepts can be used to determine the fracture parameters of cementatious material. Therefore, a number of test have been conducted to examine the applicability of LEFM to concrete. The results of those experiments show that fracture process

* 正會員, 順天大學 土木工學科 副敎授, 공학박사

● 1989. 10. 2 접수 본 논문에 대한 토론을 1990. 6. 30까지 본 학회에 보내주시면 1990. 9월호에 그 결과를 게재해 드리겠습니다.

in concrete cannot always be described with a single parameter based on LEFM bacause of significant size effect due to the formation of large fracture process zone and aggregate interlock across the crack surface.

Recently, models with more than one fracture parameter have been proposed to explain fracture process in concrete. Hillerborg et al[11] have proposed a fictitious crack model, which is more or less similar to Dugdale－Barenblatt model. Within this model, the properties of the material defined by means of one stress versus strain relation and one stress versus widening relation. If the shapes of these two curves are known, then the curves can be described by means of three parameters. The material is assumed to behave in a linear elastic manner before fracture and maximum principal fracture criterion is adopted. This makes it natural to choose the three following parameters : (1) tensile strength, (2) modulus of elasticity, (3) fracture energy. The model has been shown to correctly predict the experimentally observed size effects for notched and unnotched beam specimens.

Bazant and Cedolin[5] and Bazant and Oh[6] have proposed a crack band model based strain softening to explain the fracture process of concrete. Fracture energy, uniaxial tensile strength and width of the microcrack band are the material parameters required for crack band model.

Jenq and shah[14, 15] have proposed a two parameter model to account for size dependence in cementatious materials. Critical stress intensity factor, K^s_{IC} and Critical crack tip opening Displacement $CTOD_c$ are proposed as the two fracture criteria. The experimental results of notched beams of varing dimensions showed the proposed fracture criteria to be independent of the size of beams.

In this paper, a CLWL－DCB specimen was adopted for fracture toughness testing of concrete. The critical stress intensity factor and the critical crack tip opening displacement was calculated from the two parameter model.

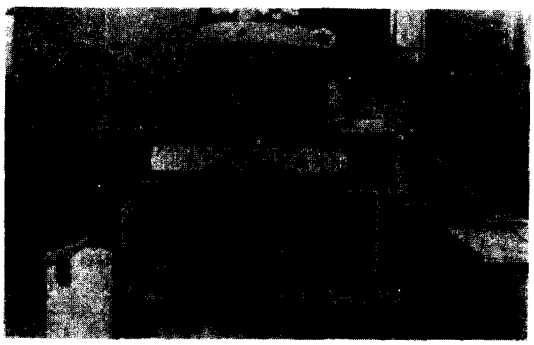

Fig. 1. Test Setup for Wedge Loading.

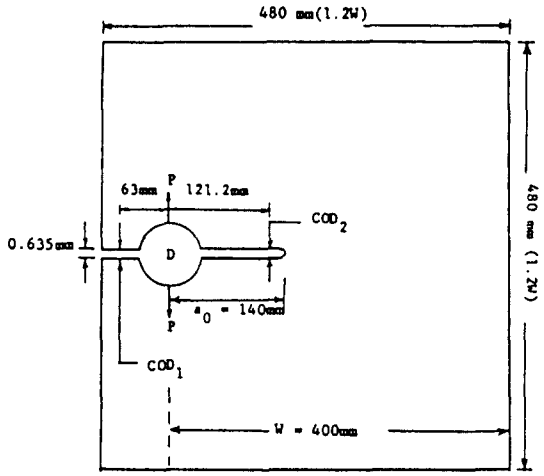

Fig. 2. Configuration of CLWL－DCB Specimen.

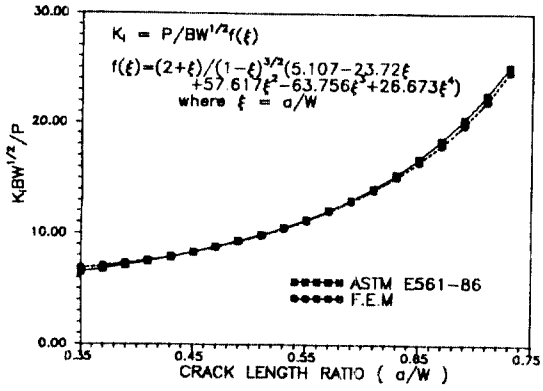

Fig. 3. Relationship between Stress Intensity Factor and Relative Crack Length

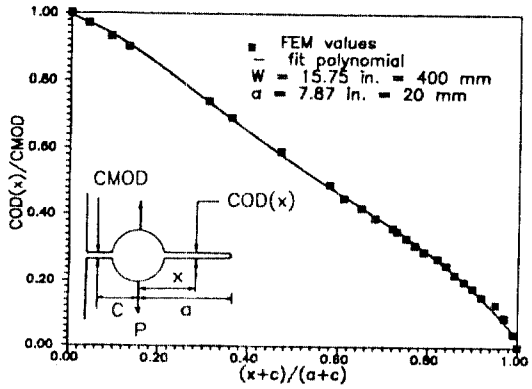

Fig. 4. Variation of Crack Opening Displacement along Crack Length

Several different types of closing pressure relationships were investigated.

Experimental Program

Testing Details

The experiments were carried in a 30 ton capacity Saginomia close-looped electric hydraulic loading system. The testing setup is shown in Fig. 1. The CLWL-DCB specimen, as shown in Fig. 2, is loaded by forcing a transverse wedge between split-pin set in loading hole. In order to monitor the crack opening load induced by the wedge, the split-pin fixture, as specified in the ASTM 561 procedure, was modified to incorporate a load cell. The crack line displacement V_1 and V_2 were measured with two clip gages.

Signal from load cell and two clip gages were amplifiedf by the strain data unit and used to chart servo mechanism. This way, the two crack line displacement could be plotted as the abscissa and ordinate, respectively. on a X-Y recorder. Surface crack length was directly measured using the replica technique developed by Hawkins et al.[4, 8, 12]

Casting and Curing

The sand and aggregate were sieved and then recombined to provide the gradations shown in table 1. The cement used was a ordinary portland cement, the fine aggregate was primarily fine grained river sand gathered in posung river and the corse aggregate was a crushed aggregate.

All the specimens were 2.4-in(60-㎜) thick, and they were cast horizontally in plywood moulds. The size for those specimens is shown in fig. 2. The loading hole was blocked out with a stainless-steel, three-inch(75㎜) diameter circular rod. This rod has a 1/4-in × 2.4-in.(6.25㎜ × 60㎜) solt along its diameter where a steel plate was inserted to form the initial notch in which the clip gages were placed during testing. The specimens were taken out of

Tabel 1. Agregate Gradation(Cumulative Percent Retained)

Crushed Gravel(for all Group)

Max. Aggregate Size	10mm	16mm	19mm
S (10mm)	100	–	–
M (16mm)	–	100	–
L (19mm)	–	–	100

Sand(for all Group)

Sieve size	No.4	No.8	No.16	No.30	No.50	No.100	Pan
Cumulative Percent	3	14	28	63	88	99	100

Fineness Modulus = 2.95

Tabel 2. Mix Proportion, Maximum Aggregate Size and material Properties for Specimen Test

No. of Specimen	Cement	Fine Aggregate	Coarse Aggregate	Water	Maximum Aggregate Size(mm)	Compressive Strength (MPa)
M2W1S1	1	3	2	0.50	10	20.6
M2W1S2	1	3	2	0.50	10	23.0
M1W1M2	1	2	1	0.40	16	30.0
M2W1M3	1	3	2	0.50	16	22.3
M2W2M4	1	3	2	0.55	16	23.2
M1W1L1	1	2	1	0.40	19	25.9
M1W1L2	1	2	1	0.40	19	25.9
M2W1L3	1	3	2	0.50	19	23.5
M2W2L1	1	3	2	0.55	19	21.6
M2W2L4	1	3	2	0.55	19	21.6

the moulds in 24hr after they were cast and placed in saturated lime water for 27 days. All the specimens and cylinder moulds were tested at an age of 28 days.

Table 2 lists the weight proportions, maximum aggregate size and compressive strength used to fabricate the specimens. The modulus of elasticity was obtained from equation given in the Buiding Code Requirements for reinforced Concrete(ACI318−83).

$$E = 0.043w\sqrt{f'_c} \quad \cdots\cdots\cdots\cdots\cdots\cdots (1)$$

where E = modulus of elasticity(MPa)

W = unit weight(8.11kg/m^3)

f'_c = compressive strength(MPa)

Finite Element Analysis

In order to analyze the experimental data, the equations for the stress intensity factor and the crack opening displacement profiles were required. So linear elastic finite element analysis using quarter−point singular element was performed. This element was first presented by Barsum[3] and Hensell and Show.[10] The progra

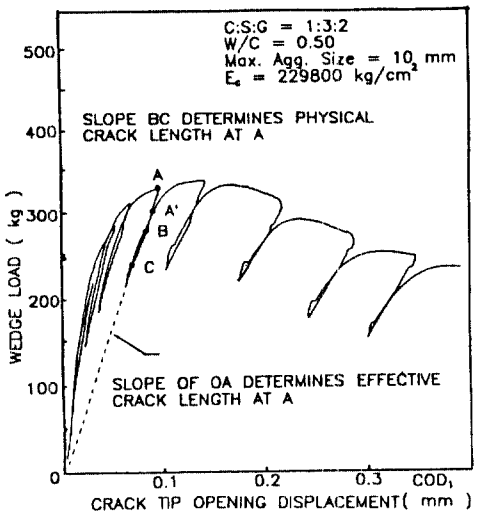

Crack End Opening Displacement

Fig. 5. Typical Load—Displacement Record

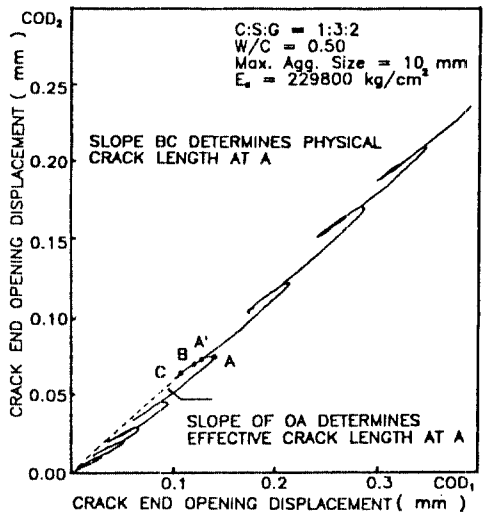

Crack End Opening Displacement

Fig. 6. Typical Double Desplacement Record.

m used in this study was developed by Jenq and Shah[13] and modified by Alvarado et al.[1] for mode I and mixed—mode fracture studies in cementatious material. Quadratic isoparametric elements which embody the inverse square root singularity are used in the calculation of stress intensity factor for the analysis.

Fig. 3. shows the plots of the stress intensity factor versus crack length ratio for the CLWL—DCB specimens. A curve of polynomial equation of stress intensity factor calculated by author gives slightly lower value than calculated by ASTME561—86[2]. The general LEFM equations required for used in this investigation for K, crack mouth opening displacement(COD $_1$), and crack tip opening displacement(COD_2), and COD are given in Appendix I. To obtain the equation for COD profile, a higher order polynomial was required to obtain sufficient accuracy. The maximum error between the polynomial and finite element results was less than 5%. In Fig, 4., a typical COD profile obtained using finite element analysis is compared with the equation given in Appendix I.

Analysis of Experimental Results

Fig. 5 show a load compliance plot relating the crack mouth opening displacement, $2V_1$, to the crack line load, measured with the load cell inserted in the split pin. A typical double displacement compliance plot from one of the test is shown in Fig. 6.

The procedures describes in ASTM 561 can be used to calculate two crack lengths for each point A on each compliance plot. The effective crack length are calculated using the slope of secant for each compliance plot. That wvalue is the elastic equivalent crack length including any nonlinear crack tip region effects for cementatious material. The effective crack length is the elastic traction free crack length

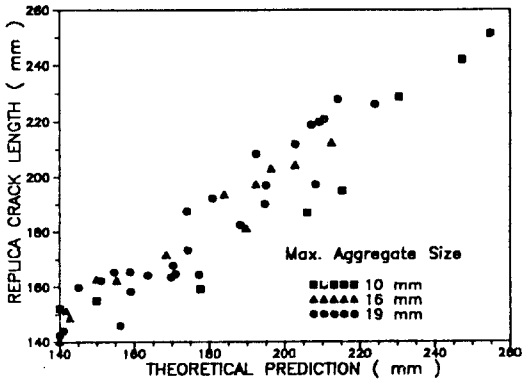

Fig. 7. Comparison Effective Crack Lenghts

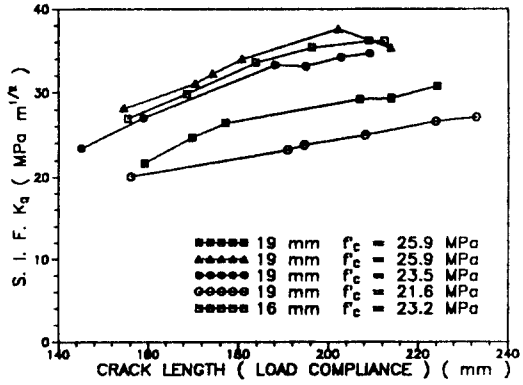

Fig. 8. R-Curve Type Relationship between Appar entFracture Toughness K_Q and Crack Length a.

augmented by any nonlinear crack tip effects caused by microcracking. The physical crack length calculated from the slope of the partial reloading curve are traction-free crack length excluding any crack tip effect.

But, it is very ambiguous to calculate the macrocrack length because difference between reloading and deloading slope at each compliance plot is nearly zero. So, the effective crack length are only calculated using the slope of secant for each compliance plot in this study.

A comparison of replica measured crack extension with the corresponding values of theoretically predicted value is shown in Fig.7. Theoretical values are the effective crack length. The theoretical crack extension is slightly larger than the replica crack extension.

Two Parameter Model Analysis

To calculate the effective crack growth at the point of unloading, first the initial slope of load versus crack opening displacement plot used to calculate the Young's modulus E. Eq. 7 and 8 (Appendix I) are combined to obtain

$$E = \frac{P}{COD}\cdot\frac{1}{B}\cdot\frac{a}{W}\cdot F_1\left(\frac{x+c}{a+c},\ \frac{a+c}{W+c}\right) \quad \cdots\cdots\cdots\cdots\cdots (2)$$

Notation are defined in Appendix I. Once the calculation of the modulus of elasticity E is obtained, then effective crack length can be calculated by using Eq. 2 and value of load compliance was experimentally measured. The value of stress intensity factor K_Q, often called the apparent fracture toughness, for the point of unloading can be calculated from Eq. 6 (Appendix I) using the measured load and the value of effective crack length.

Fig. 8 shows a plot of K_Q versus effective crack length calculated from the analysis of forementioned two compliance plot. The data point of four specimens are shown in Fig. 8. There is no evidence of K_Q reaching asymptotic value or plateau with crack extension. R-curves are not suitable for predicting the onset of unstable cracking for concrete specimens tested in this study.

To predict the critical load for CLWL specimens, the critical stress intensity factor and cri

Table 3. K^S_{IC} and $CTOD_C$ Value Obtained from CLWL-DCB Specimens

Max. Agg. Size	f'_c(MPa)	a_e/W	K^S_{IC}(MPa $m^{1/2}$)	$CTOD_C$(mm)
10 mm	23.0	0.440	0.729	0.011
10 mm	20.6	0.557	0.790	0.010
16 mm	23.2	0.383	0.932	0.015
16 mm	22.3	0.443	1.160	0.015
16 mm	30.2	0.452	1.045	0.013
19 mm	21.6	0.427	1.029	0.014
19 mm	21.6	0.441	0.714	0.010
19 mm	23.5	0.459	1.100	0.009
19 mm	25.9	0.357	0.966	0.022
19 mm	25.9	0.460	0.946	0.027

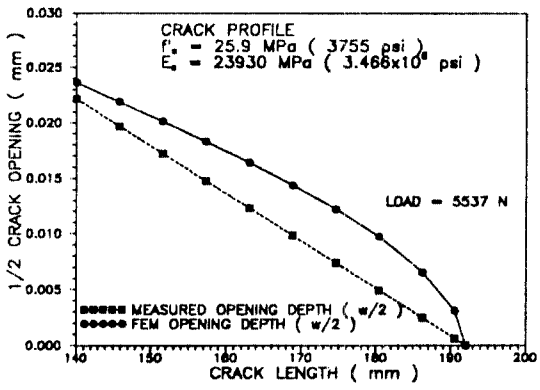

Fig. 9. Comparisons of the Experimental Crack Profiles and the LEFM Solution

tical crack tip opening displacement are calculated using the two parameter model. Table 3 gives a brief summary of the fracture parameters obtained for the specimen tested here. The critical stress intensity factor ranges from 0.714 MPa $m^{1/2}$ to 1.16 MPa $m^{1/2}$. The values of $CTOD_C$ have a tendency to increse in proportion to maximum aggregate size and are 0.009-0.027mm for concrete. It can be noticed that K^S_{IC} and $CTOD_C$ are very similar to the values obtained from wedge splitting data. It is, however, not clear that critical stress intensity factor and crack tip opening displacement are fracture parameter that have not effected by the size or geometry. Therefore, a larger number of specimen and larger variation of original notch length ratio are needed to reach the definite conclusion.

Consideration of Cohesive Crack Model

The superposition method[16] was used to obtain the closing pressure-crack opening relationship(σ-w) required for the analytical crack profiles to match the measured profiles. During this analysis an finite element program developed by Jenq and shah[13] and modified by author was used. The program used quadratic eight node quarter point singular element to account for the singularity at the crack tip.

The clip gage displacement(COD_1) and the actual crack length measured by replica technique are used to calculate the measured crack profiles. Authors assumed that displacement at any point along the crack is linearly changed to depend on the crack length.

A unit closing force was applied at each node along the crack faces and its corresponding node across the crack. The nodal displacement long the crack produced by each unit force are one row of the compliance matrix C that relates closing forces $\underline{f}$ and closing displcements $\delta\underline{W}$.

$$\delta\underline{W} = \underline{c}\,\underline{f} \quad \cdots\cdots\cdots\cdots\cdots\cdots \quad (3)$$

where $\delta\underline{W}$ is a difference between LEFM crack profiles $\underline{W}_e$ and the measured crack profiles $\underline{W}_m$ shown in Fig. 9.

From Eq. 3, the nodal force corresponding to closing pressure $\underline{f}$ are represented by

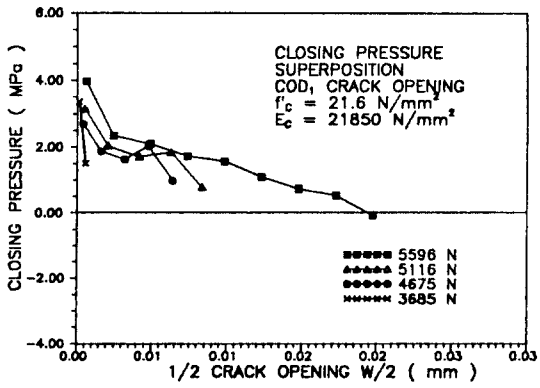

Fig. 10. Superposition Closing Pressure obtained from COD_1

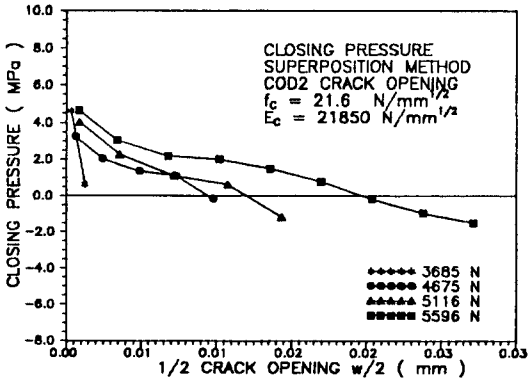

11. Superposition Closing Pressure obtained from COD_2

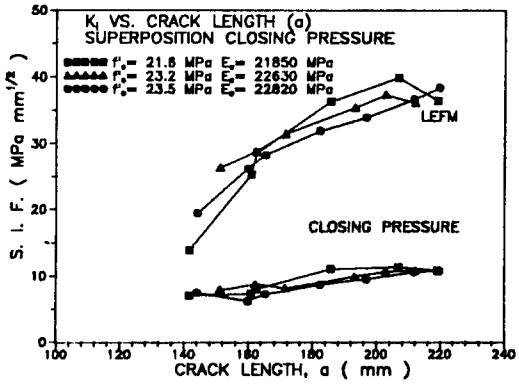

Fig. 12. Comparison of LEFM Stress Intensity Factor K_{Ie} and Superposition Method Stress Intensity Factor K_I for Various Crack Length

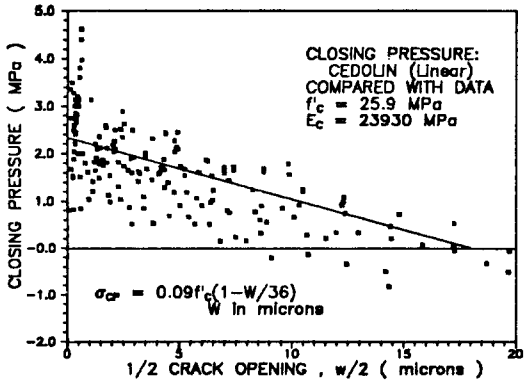

Fig. 13. The Closing Pressure—Crack Opening Displacement Relationship represented with Linear Curve.

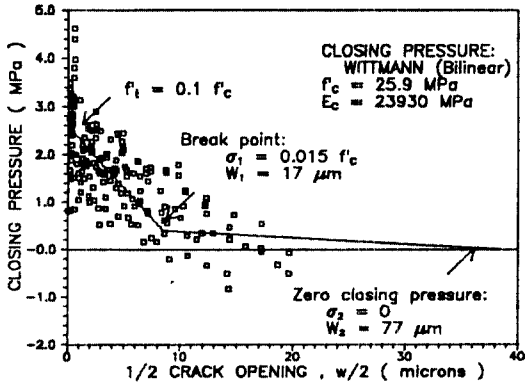

Fig. 14. The Closing Pressure—Crack Opening Displacement Relationship represented with Bilinear.

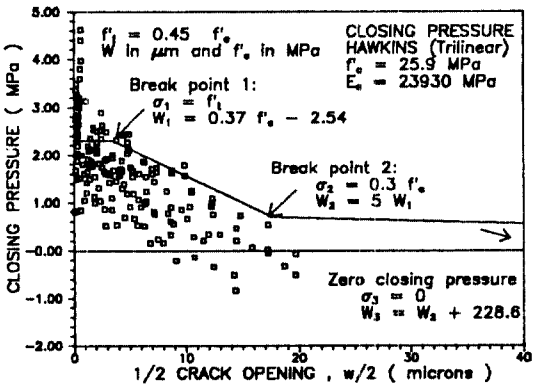

Fig. 15. The Crack Closing Pressure—Crack Opening Displacement Relationship represented with Trilinear.

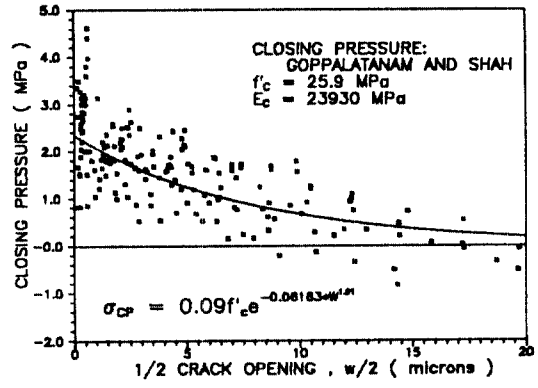

Fig. 16. The Closing Pressure—Crack Opening Displacement Relationship represented with Exponential Curve.

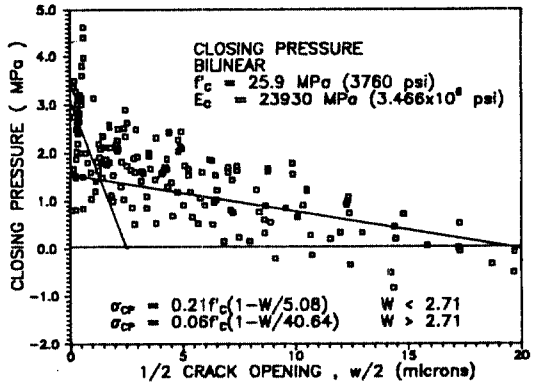

Fig. 17. The Closing Pressure—Crack Opening Displacement Relationship represented with Bilinear.

$$\underline{f} = \underline{C}^{-1}(\underline{W}_e - \underline{W}_m) \quad \cdots\cdots\cdots\cdots\cdots\cdots \quad (4)$$

Fig. 10 and 11 show the superposition closing pressures obtained from COD_1 and COD_2 crack profiles, respectively, for the various crack lengths.

Mode I crack intensity factor corresponding to each unit force was computed to obtain the stress intensity coefficient $\underline{k}$. The total stress intensity factor for any set of closing force f is

$$K_I = K_{Ie} - \underline{f}^T\underline{k} \quad \cdots\cdots\cdots\cdots\cdots\cdots \quad (5)$$

Fig. 12 shows the LEFM stress intensity factor K_{Ie} and the superposition stress intensity factor K_I for various crack lengths. K_I has an upper bound of 13.0 MPa $mm^{1/2}$. This value is very close to the stress intensity factor obtained from th holographic crack profiles by Miller et al.[16] The upper bound is of interest because one cannot be sure that measurements are made just before crack propagation, thus lower values are expected. Therefore, the fact that the upper bound is constant suggest that there is a material property K_{IC}.

Some reserchers have proposed colsing pressure versus crack opening displacement relationships.

The question whether or not it is possible to calculate a closing pressure exactly for all crack length is of great importance. Therefore, five closing pressures were compared with a closing pressures data obtained in this study :

1) Linear. Proposed by Cedolin, Iori and Dei Pori[7](Fig. 13)

2) Bilinear. Proposed by Roelfstra and Wittmann[17](Fig. 14)

3) Trilinear. Proposed by Jeang and Hawkins[12](Fig. 15)

4) Exponential. Proposed by Gopalaratnam and Shah[9](Fig. 16)

5) Bilinear. Proposed by Miller, Castro and Shah[16](Fig. 17)

Fig 13 and 15 shows that those closing pressures are almost upper bound of superpositon results. Fig. 14, 16 and 17 shows that those closing pressure are a good fit to the values obtained by superposition method.

CONCLUSIONS

1. An effective crack length approach may be used to analyze the nonlinear response of concrete.

2. It was confirmed that surface crack length can be accurately measured by replica technique using Acetylcellulose film.

3. Crack resistance used for the measurement of stable crack growth increased in proportion to maximum aggregate size and concrete strength. it was, however, found that the precise predicting of the point of onset of unstable crack was difficult.

4. Using the superpostition method, it is possible to find closing pressure versus crack opening displacement relationships.

5. The superposition method suggests that a value of K_I = 13.0 MPa $\sqrt{m}$ may be an appropriate value for the fracture toughness of the concrete studied.

ACKNOWLEDGEMENT

This reaserch was supported by the Professor Training Program of the Korean government.

APPENDIX I. LEFM based Equations

1. LEFM based equations for CLWL-DCB specimens. Stress Intensity Factor(K_I)[2] :

$$K_I = \frac{P}{BW} F\left(\frac{a}{W}\right) \qquad (6)$$

$$F\left(\frac{a}{W}\right) = \frac{(2+A)(0.866+4.64A-13.32A^2+14.72A^3-5.6A^4)}{(1-A)^{3/2}}$$

where A = a/W ; and a W are defined in Fig. 2.

Crack mouth opening displacement(CMOD or COD_1)[2] :

$$CMOD = \frac{P}{BE'} V\left(\frac{a}{W}\right) \qquad (7)$$

where $E' = E/(1-\mu^2)$ for plane strain ; for plane stress ; E = Young's modulus of elasticity and

$$V\left(\frac{a}{W}\right) = 101.9-948.9A+3691.5A^2-6064.W1A^3+4054.1A^4$$

Crack opening displacement(COD) (curve fitting of numerical results based on finite element method)

The general form is

$$COD(x) = CMOD \cdot F_1\left(\frac{x+c}{a+c}, \frac{a+c}{W+c}\right) \quad (8)$$

$$COD(x) = CMOD[1+(3.171A+0.581)B+(8.011A-5.639)B^2+(-7.313A+6.365)B^3+(2.482A-2.308)B^4]^{1/2}$$

where $A = (x+c)/(a+c)$; $B = (W+c)$; x = distance from the center of pin hole in plate at which the COD is desired ; c = distance from the loading point to point at CMOD was measured(6.3㎜) ; a = effective crack length ; W = characteristic length of the specimen(400 ㎜)

APPENDIX II. REFERENCES

1. Alvarado, M. A., Shah, S. P., and John, R., "Mode I Fracture in Concrete using Center-Cracked Plate Specimens", *Journal of Engineering Mechanics*, Vol. 115, No. 2, Feb., 1989, pp. 366-383.
2. "ASTM E561-86, Standard Practice for R-Curve Determination," *Annual Book of Standards, American* Society of Testing Materials, Part 10, 1986.
3. Barsum, R. S., "On The Use of Isoparametric Finite Elements in Linear Fracture Mechanics," *International Journal for Numerical Method in Engineering, Vol. 10, pp. 25-30, 1976.*
4. *Barker, D. B., Hawkins, N. M., Jeang, F. L., Cho, K. Z., and Kobayashi, A. S., "Concrete Fracture in CLWL Specimen," Journal of Engineering Mechanics, Vol. 111, No. 5, May, 1985, pp. 623-637.*
5. *Bazant, Z. P., and Cedolin, L., "Blunt Crack Band Propagation in Finite Element Analysis," Journal of the Engineering Mechanics,* Vol. 106, No. EM6, Dec., 1980. pp. 1287-1306.
6. Bazant, Z. P., and Oh, B. H., "Crack Band Theory for Fracture of Concrete", *Materiaux et Constructions*, Vol. 16, No. 93, May-June, 1983, pp. 155-177.
7. Cedolin, L., Deipoli, S., and Iori, I., "Tensile Behavior of Concrete," *Journal of Engineering Mechanics*, Vol. 113, No. 3, p. 431, 1987.
8. Cho, K. Z., Kobayashi, A. S., Hawkins, N, M., Barker, D. B., and Jeang F. L., "Fracture Process Zone in Concrete Cracks," *Journal of the Engineering Mechanics*, Vol, 110, No. 8, August, 1984, pp. 1174-1183.
9. Gopalaratnam, V. S., and Shah, S. P., "Softening Response of Plain Concrete in Direct Tension," *ACI Journal of Materials Reserch*, Vol. 2, No. 3, 1987, pp. 345-356.
10. Hensell, R. D. and Shaw, K. G., "Crack Tip Finite Elements are Unnecessary," *International Journal for Mumerical Nethods in Engineering*, Vol. 9, pp. 495-507, 1975.
11. Hillerborg, A., Modeer, M., and Peterson P. E., "Analysis of a Crack Formation and Growth in Concrete by Means of Fracture Mechanics and FiniteElements," *Cement and Concrete Research*, Vol. 6, No. 6, 1987, pp. 773-782.
12. Jeang, F. L. and Hawkins, N. M., "Nonlinear Analysis of Concrete Fracture," *Structure and Mechanics Report, Department of Civil Engineering, University of Washingtion, Seattle, Washington, 1985.*
13. *Jenq, Y. S.*, "Fracture Mechanics studies of Cementitious Conposites," *thesis presented to the Department of Civil Engineering, Northwestern University, at Evanston, Ill., in partial fullfillment of the require-*

ments for the Degree of Doctor of Philosophy.

14. *Jenq, Y. S, and Shah, S. P.*, "*Fracture Toughness Criterion for Concrete*," *Engineering Fracture Nechanics*, Vol. 21, No. 5, 1985, 1055－1069.
15. Jenq, Y. S, and Shah, S. P., "Geometrical Effects on Mode I Fracture Parameters," Technical Report, Department of Civil Engineering, Northwestern University, 1989.
16. Miller, R. A., Castro, A., and Shah, S. P., "Cohesive Crack Models Examined with Laser Holography" Measurements", Dept, of Civil Engineering, Northwestern University, 1989.
17. Roelfstra, R. E., and Torrent, R. H., "The Effect of the Shape of the Strain Softening with Fracture of Concrete," *Fracture Tousghness and Fracture Energy of Concrete*, F. H. Wittmann Editor., Elsevier Science Publishers, B. V., Amsterdam, 1986.